This is the accepted manuscript made available via CHORUS. The article has been published as:

Kinetic Theory and Vlasov Simulation of Nonlinear Ion-Acoustic Waves in Multi-Ion Species Plasmas

T. Chapman, R. L. Berger, S. Brunner, and E. A. Williams

Phys. Rev. Lett. **110**, 195004 — Published 10 May 2013

DOI: 10.1103/PhysRevLett.110.195004

Kinetic theory and Vlasov simulation of nonlinear ion acoustic waves in multi-ion species plasmas

T. Chapman,[1,*] R. L. Berger,[1] S. Brunner,[2] and E. A. Williams[1]

[1]*Lawrence Livermore National Laboratory, P.O. Box 808, Livermore, CA 94551, USA*
[2]*Centre de Recherches en Physique des Plasmas, Association EURATOM-Confédération Suisse, Ecole Polytechnique Fédéral de Lausanne, CRPP-PPB, CH-1015 Lausanne, Switzerland*

(Dated: March 6, 2013)

The theory of damping and nonlinear frequency shifts from particles resonant with Ion Acoustic Waves (IAWs) is presented for multi-ion species plasma and compared to driven wave Vlasov simulations. Two distinct IAW modes may be supported in multi-ion species plasmas, broadly classified as fast and slow by their phase velocity relative to the constituent ion thermal velocities. In current fusion-relevant long pulse experiments, the ion to electron temperature ratio, $T_\mathrm{i}/T_\mathrm{e}$, is expected to reach a level such that the least damped and thus more readily driven mode is the slow mode, with both linear and nonlinear properties that are shown to differ significantly from the fast mode. The lighter ion species of the slow mode is found to make no significant contribution to the IAW frequency shift despite typically being the dominant contributor to the Landau damping.

PACS numbers:

The kinetic damping of large-amplitude, low-frequency waves in multi-ion species plasma plays an essential role in Inertial Confinement Fusion (ICF). In ignition experiments at the National Ignition Facility (NIF), gold-boron and helium-hydrogen mixtures were proposed to increase the Landau damping of Ion Acoustic Waves (IAWs) and, thereby, to suppress the growth of Stimulated Brillouin Scattering (SBS) [1]. In addition to its low atomic number, high density and a host of manufacturing considerations, CH was chosen as the standard ablator material for NIF ignition capsules in part because of concern that, as the plasma ablated from the capsule streamed into the path of the laser, IAWs in a pure beryllium or diamond (HDC) plasma would backscatter via SBS more light than in a CH plasma [2]. When significant energy is transferred to IAWs, trapping of particles in the wave potential may produce a non-Maxwellian distribution, reducing Landau damping [3] and potentially eliminating the higher IAW damping of the multi-ion species plasmas.

In this Letter, we address two distinct ion acoustic modes in a two-ion species plasma, which have been observed in dedicated scattering experiments [4]. One of these modes, known as the slow mode (defined fully later), has a phase velocity nearly equal to the ion thermal velocity of the lighter ion species. Plasma wave modes with phase velocities close to the thermal velocity of one of the plasma species, broadly classified as slow waves, are of universal interest in plasma physics. A slow mode qualitatively similar to that addressed in this Letter present in single-ion species plasmas has been produced recently in laboratory experiments [5].

This Letter provides the first examination of the complex nonlinear behaviour of multi-ion species IAWs as the wave amplitude and ion to electron temperature ratio $T_\mathrm{i}/T_\mathrm{e}$ are varied, the understanding of which are necessary for modeling of SBS and interpreting SBS experiments and thus for selecting optimal ICF hohlraum materials. In NIF ignition experiments [6], T_e in the path of the laser beam exceeds 2 keV and T_i approaches $T_\mathrm{e}/2$ at peak laser power. Via SBS, IAWs may grow and scatter significant laser energy away from the desired path in ICF experiments, impeding the ablation process necessary for ignition. The question of which IAW mode is least damped thus becomes of great importance in understanding the behaviour of SBS. As $T_\mathrm{i} \to T_\mathrm{e}$, the least damped mode is the slow mode, with phase velocity close to the H ion thermal velocity [7]; this property of the slow mode of CH holds for all physically relevant $T_\mathrm{i}/T_\mathrm{e}$, but is applicable also for C/H number fractions as low as $\sim$0.01 and for the slow modes of a diverse range of plasmas. In space plasmas, values of $T_\mathrm{i}/T_\mathrm{e}$ of order 1 are common, and slow modes have been suggested as an important source of observed turbulence in the solar wind [8].

Previously, we showed for a single-ion species plasma the importance of including the kinetic contribution of the electrons and harmonic generation to describe IAWs driven to a nonlinear BGK-like equilibrium state [9]. There, we found that the ions of charge number Z provided the dominant damping in the linear state and the dominant contribution to the Kinetic Nonlinear Frequency Shift (KNFS) in the BGK-like state if $ZT_\mathrm{e}/T_\mathrm{i} \lesssim 10$. Based on these results, one might expect for a CH plasma that the H ions with $Z = 1$ would provide the dominant frequency shift in the nonlinear state. However, the theory and Vlasov simulations of KNFSs for fast and slow modes presented here show that the H ions play almost no role in the KNFS of the slow mode; average-charge ion models of multi-ion species plasmas (where the plasma is simplified to a single ion species) may be misleading in both the magnitude and sign of the KNFS. It will also be shown by comparison of theory and

Vlasov simulations that the distribution function for all species of the least damped mode is best represented by an adiabatic one (to be specified clearly later), in contrast to single-ion species simulation results [9] (where the ions were found to be excited non-adiabatically as T_i approaches T_e). In the regime considered here, both harmonic generation and kinetic wave-particle interactions are required to achieve quantitative agreement between theoretical models of the nonlinear IAW frequency and Vlasov simulations. While we address the physically relevant case of CH, these findings are applicable to many multi-species plasmas.

We consider a neutral, unmagnetized, fully-ionized CH plasma (50:50 mix) with equal ion species temperatures ($T_\mathrm{H} = T_\mathrm{C} = T_\mathrm{i}$). The ion species in multi-ion modes are typically characterized by their thermal velocities $v_\mathrm{th,i}$ relative to the phase velocity v_ϕ of an IAW of wave number k and frequency ω, where $v_\phi = \mathrm{Re}[\omega]/k$, $v_\mathrm{th,i} = \sqrt{T_\mathrm{i}/m_\mathrm{i}}$, and m_i is the mass of an ion species. IAW modes are loosely classified as "fast" when $v_\phi > v_\mathrm{th,1,2}$ and "slow" when $v_\mathrm{th,1} > v_\phi > v_\mathrm{th,2}$ (in our example, species 1 is the "light" H and 2 is the "heavy" C). The properties of an IAW mode, including its phase velocity and Landau damping, are dependent on the relative fractions and mass ratios of the ion species and on $T_\mathrm{i}/T_\mathrm{e}$. Across the parameter space of interest, the ion and phase velocities of the fast mode of CH are all well-separated. The so-called slow mode, however, has a value close to unity of the ratio $v_\phi/v_\mathrm{th,H}$ that is only weakly dependent on $T_\mathrm{i}/T_\mathrm{e}$, making conventional analytic treatments of the slow mode difficult.

The multi-species, linear kinetic dispersion relation for one dimensional (1D) longitudinal plasma waves in a non-magnetized, homogeneous plasma is given by,

$$\epsilon_\mathrm{L}(\omega,k) = 1 + \sum_{\text{species}} \chi_j = 0,\ \chi_j = \frac{1}{(k\lambda_{\mathrm{D},j})^2} W(z_j), \quad (1)$$

where χ_j is the susceptibility of species j (electron, H ion or C ion) with density N_j, charge number Z_j, temperature T_j and mass m_j, for which $\lambda_{\mathrm{D},j}^2 = v_{\mathrm{th},j}^2/\omega_{\mathrm{p},j}^2$, $v_{\mathrm{th},j}^2 = T_j/m_j$, $\omega_{\mathrm{p},j}^2 = N_j Z_j^2 e^2/m_j\varepsilon_0$, and $z_j = \omega/kv_{\mathrm{th},j}$. e is the magnitude of the electron charge and ε_0 is the permittivity of free space. W is the dispersion function,

$$W(z) = \frac{1}{\sqrt{2\pi}} \int_{\bar{v}_j} d\bar{v}_j \, \frac{\bar{v}_j}{\bar{v}_j - z} \exp(-\bar{v}_j^2/2), \quad (2)$$

where $\bar{v}_j = v/v_{\mathrm{th},j}$, z is generally complex and a Maxwellian velocity distribution for all species is assumed. The dispersion relation $\epsilon(\omega,k) = 0$ relates ω to k for any given electrostatic normal mode.

Using the parameters discussed earlier, W may be approximated straight-forwardly and an analytic expression found when $|z| \ll 1$ (e.g. by Taylor expansion of W, here valid for the electrons) or $|z| \gg 1$ (W may be expressed as an asymptotic series, valid to reasonable accuracy for the heavy C ions). Since for the H ions in the slow mode $|z_\mathrm{H}| \sim 1$, neither these approximations nor multi-pole expansions of W work well over the regime of interest (see Ref. [7] and references therein for further detail). Direct numerical solutions to Eq. (1) are shown in Fig. 1a for the fast and slow modes, lying at inter-

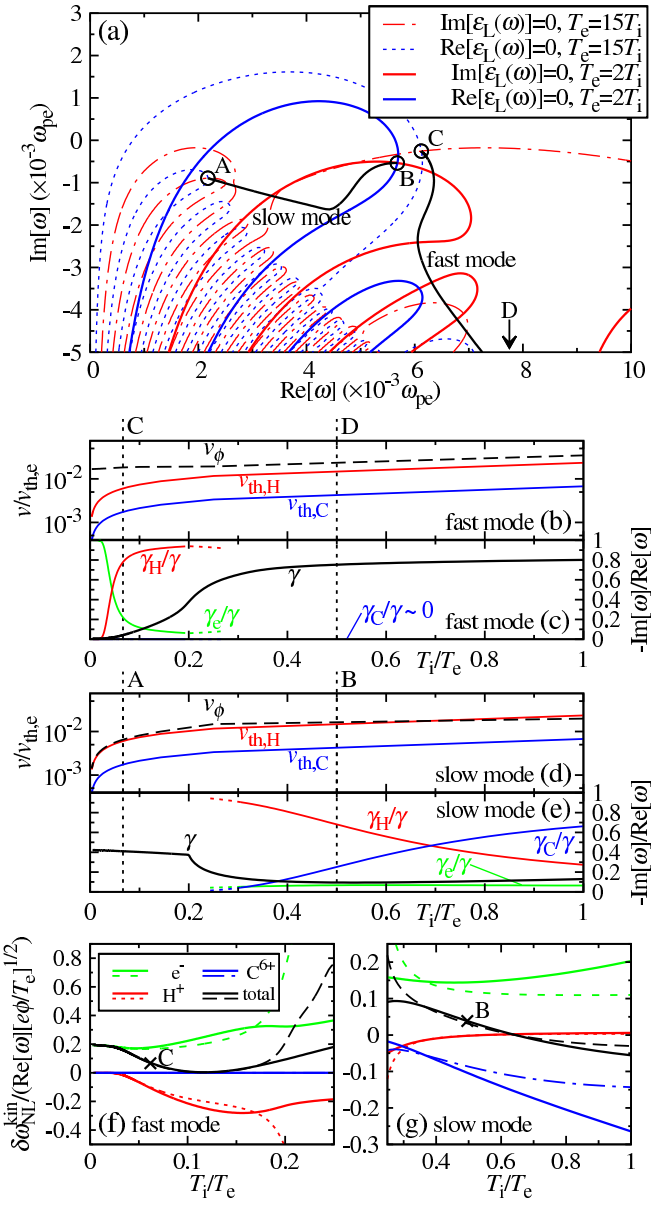

FIG. 1: (a) Contours of solutions to the slow and fast IAW mode dispersion relations for $k\lambda_{\mathrm{D,e}} = 1/3$. As the ratio $T_\mathrm{i}/T_\mathrm{e}$ increases from 1/15 to 1/2, the frequency of the slow mode moves from A to B and the fast mode from C to D. Below, the (b)/(d) mode phase velocities, (c)/(e) total damping decrement, fractional damping due to each species, and (f)/(g) kinetic nonlinear frequency shift assuming adiabatic wave excitation for all species (solid lines: ϵ_R=Re[ϵ_L(Re[ω], k)]; patterned lines: ϵ_R=Re[$\epsilon_\mathrm{L}(\omega, k)$]).

sections of zero contours of the real and imaginary parts of $\epsilon(\omega, k\lambda_{\mathrm{D,e}} = 1/3)$, where $\lambda_{\mathrm{D,e}}$ is the electron Debye length (used throughout this Letter, $k\lambda_{\mathrm{D,e}} = 1/3$ is typical of SBS experiments, although kinetic effects are only weakly dependent on this parameter). There are an infinite number of such intersections, each having different Landau damping decrements $\gamma = -\mathrm{Im}[\omega]/\mathrm{Re}[\omega]$; we refer to as "the slow mode" and "the fast mode" the least damped modes belonging to each class of mode.

Figures 1b-1e show the phase velocity and damping corresponding to the fast and slow modes as a function of $T_\mathrm{i}/T_\mathrm{e}$; the slow mode is less damped than the fast for $T_\mathrm{i}/T_\mathrm{e} \gtrsim 0.2$, and is thus preferentially driven in this regime near the SBS threshold. It is interesting to ask: which species contributes most to the damping? In the resonant approximation (assuming $\mathrm{Im}[\omega]/\mathrm{Re}[\omega] \ll 1$), Eq. (1) may be solved to lowest order to yield the following analytic expression for the linear Landau damping, relevant to multi-species plasma waves:

$$\tilde{\gamma} = \sum_{\text{species}} \tilde{\gamma}_j \approx \beta_\gamma \sum_{\text{species}} \frac{1}{\tilde{v}_{\mathrm{th},j}\tilde{\lambda}_{\mathrm{D},j}^2} \exp\left(-z_j^2/2\right), \quad (3)$$

where $\beta_\gamma = \sqrt{\pi/2}\tilde{\omega}_\mathrm{R}\tilde{k}^{-3}(\partial\epsilon_\mathrm{R}/\partial\tilde{\omega}_\mathrm{R})^{-1}$, $\omega_R = \mathrm{Re}[\omega]$ and $\epsilon_\mathrm{R} = \mathrm{Re}[\epsilon_\mathrm{L}]$ (ϵ_R is discussed later). Tilde denotes normalization to electron quantities $\lambda_{\mathrm{D,e}}$, $v_{\mathrm{th,e}}$, $\omega_{\mathrm{p,e}}$, and T_e, as appropriate. For the electrons in an IAW, $\tilde{\gamma}_e/\beta_\gamma \approx 1$. Using Eq. (3), the fractional contribution of each species to the total damping is plotted in Figs. 1c and 1e (the restricted plotted range corresponds to the limits of the resonant approximation). Thus, across the regimes of physical interest (i.e. the more weakly damped regimes of each mode), the electrons contribute most to the damping of the fast mode for $T_\mathrm{i}/T_\mathrm{e} \lesssim 0.04$ and the H ions for $T_\mathrm{i}/T_\mathrm{e} \gtrsim 0.04$, while the H ions dominate the damping of the slow mode for $T_\mathrm{i}/T_\mathrm{e} \lesssim 0.7$ and the C ions for $T_\mathrm{i}/T_\mathrm{e} \gtrsim 0.7$.

The travelling potential ϕ of a plasma wave, propagating at the phase velocity v_ϕ, traps particles within the plasma with velocities close to v_ϕ. This trapping, in addition to suppressing Landau damping [3], leads to a nonlinear frequency shift $\delta\omega_\mathrm{NL}^\mathrm{kin}$ away from ω_R (referred to previously as the KNFS). Each species in the plasma makes a contribution to this effect, the significance of which is dependent upon the plasma parameters. Simple analytic expressions in which $\delta\omega_\mathrm{NL}^\mathrm{kin}$ is proportional to the square root of the potential amplitude have been derived in the sudden [10, 11] and adiabatic limits [11] of wave generation (these derivations are for the case of a Langmuir wave, but were shown to apply to IAWs in Ref. [9]), the latter being the more relevant to stimulated scattering processes and the conditions discussed here. Following this methodology, one finds for a multi-species plasma wave in the resonant approximation with Maxwellian distributions,

$$\delta\tilde{\omega}_\mathrm{NL}^\mathrm{kin} = -\beta_\omega|\tilde{\phi}|^{1/2} \sum_{\text{species}} \alpha_j \frac{1}{\tilde{\lambda}_{\mathrm{D},j}^2}\left(\frac{|Z_j|}{\tilde{T}_j}\right)^{1/2} K(z_j), \quad (4)$$

where $\beta_\omega = \sqrt{2/\pi}\tilde{k}^{-2}(\partial\epsilon_\mathrm{R}/\partial\tilde{\omega}_\mathrm{R})^{-1}$, $\tilde{\phi} = e\phi/T_\mathrm{e}$, α_j is a constant with a value dependent on how the species within the wave was excited (for adiabatic excitation, $\alpha_j{=}\alpha_\mathrm{ad}{\equiv}0.544$; for sudden excitation, $\alpha_j{=}\alpha_\mathrm{sud}{\equiv}0.823$ [11]), and the sign of the contribution of each species to the total KNFS is determined by $K(z_j) \equiv \left(z_j^2 - 1\right)\exp\left(-z_j^2/2\right)$.

Figures 1f and 1g plot Eq. (4) for the fast and slow wave, respectively ($\alpha_\mathrm{e}{=}\alpha_\mathrm{H}{=}\alpha_\mathrm{C}{=}\alpha_\mathrm{ad}$, justified by Vlasov simulations shown later, and $\partial\epsilon_\mathrm{R}/\partial\omega_\mathrm{R}$ is evaluated numerically). Over the physically relevant (weakly-damped) range of $T_\mathrm{i}/T_\mathrm{e}$ for each species, several features are apparent. For both the fast and the slow modes examined here, the positive frequency shift due to the electrons opposes and is of greater magnitude than the negative shift due to the ions, thus computationally lighter Boltzmann fluid models of electrons favoured in many past studies of IAWs would give incorrect results as they neglect electron trapping; the full kinetic behaviour of electron and ion species must be captured, as established in Ref. [12] for particle-in-cell simulations. One sees immediately from Fig. 1d that for the H ions of the slow mode, $K(z_\mathrm{H}) \approx 0$, i.e. H ions make a negligible contribution to the KNFS [13], yet contribute most to Landau damping in the linear limit; the C ions however make a significant contribution to the KNFS. In contrast, H ions in the fast mode provide a significant contribution to the KNFS, while the C ions with $v_{\mathrm{th,C}} \ll v_\phi$ (see Fig. 1b) are negligible for both the KNFS and the linear Landau damping.

In the derivation of $\delta\omega_\mathrm{NL}^\mathrm{kin}$ in Refs. [10] and [11], it is seemingly ambiguous as to whether one should take $\epsilon_\mathrm{R} = \mathrm{Re}[\epsilon_\mathrm{L}(\mathrm{Re}[\omega], k)]$ or $\epsilon_\mathrm{R} = \mathrm{Re}[\epsilon_\mathrm{L}(\omega, k)]$ (this is discussed in detail in Ref. [9]). Outside of the weakly damped region for each mode, as $\mathrm{Im}[\omega]$ approaches $\mathrm{Re}[\omega]$, Eqs. (3) and (4) differ greatly depending on the choice of ϵ_R made, giving results that are unphysical over certain ranges. However, within the weakly damped regimes for both modes, where the resonant approximation is valid, the choice of ϵ_R is of limited importance, as seen in Figs. 1f and 1g (in the following weakly damped cases, $\epsilon_\mathrm{R} = \mathrm{Re}[\epsilon_\mathrm{L}(\mathrm{Re}[\omega], k)]$ is chosen).

In order to investigate the physics described previously, the code SAPRISTI was used (described in Ref. [9]), which solves the full Vlasov-Poisson system for electrons as well as multiple ion species using a semi-Lagrangian scheme and retaining one dimension in space and velocity (1D1V). By restricting the simulation size to a single wavelength (composed of 128 spatial mesh points) with periodic boundary conditions, processes such as IAW decay and modulational instability were prevented from oc-

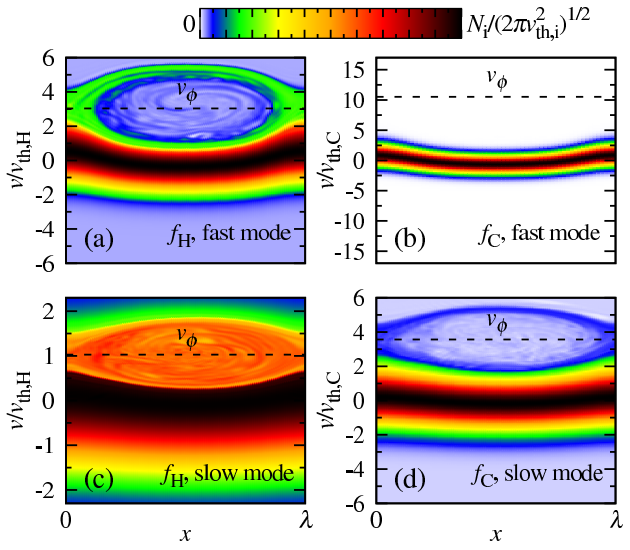

FIG. 2: Ion distributions from Vlasov simulations for the fast and slow modes after an undriven BGK-like mode has been established. Here, $\tilde{\phi} \sim 0.1$ for both modes.

curring, allowing the precise analysis of the frequency of the nonlinear wave in isolation. To resolve the electron kinetic behaviour, a time step of $0.1\omega_{\mathrm{p,e}}^{-1}$ was used. A minimum of 50 mesh points across the steady-state trapping velocity width were ensured, with a typical total of 512 uniformly spaced velocity mesh points for the electrons and 1024 for each of the ion species over the species velocity range $[-6v_{\mathrm{th},j}, +6v_{\mathrm{th},j}]$.

In simulations, an IAW was excited at its linear frequency from an initially Maxwellian distribution using a prescribed ponderomotive driver, applied to the electrons as an external field in the Vlasov equation of strength $eE_{\mathrm{driver}}/\lambda_{\mathrm{De}}T_{\mathrm{e}} = 1\times10^{-3}$, that ensured growth was slow on the time scale of the ion plasma and ion bounce frequency, $\omega_{\mathrm{b,i}} = k(Z_i e\phi/m_i)^{1/2}$. After establishing the direction of the frequency shift of the mode by driving at a fixed frequency in test cases, the driver was then swept slowly in frequency from the linear mode frequency in the direction of the observed frequency shift to prevent detuning of the IAW which, without applying a very strong driver, would otherwise prevent larger IAW amplitudes from being obtained. Such a process allows phase-locking of the mode to the driver, known as autoresonance, and thus does not require feedback to maintain resonance. After the desired amplitude was reached (taking times of the order of $10^5\omega_{\mathrm{p,e}}^{-1}$), the driver was switched off and the IAW allowed to propagate freely. Measurements of particle distributions (Fig. 2) and nonlinear frequency shifts (Figs. 3c,d) were made after a BGK-like mode [14] had been established due to trapping. The shift $\delta\omega_{\mathrm{NL}}$ was determined by comparing the time-asymptotic state of the free IAW to an IAW of zero amplitude (extrapolated from the lowest measured amplitude cases), and

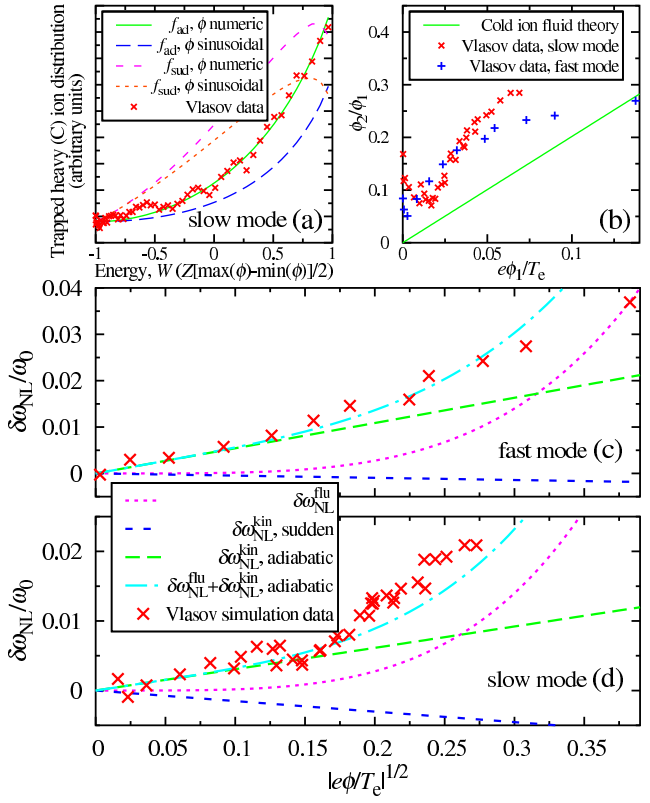

FIG. 3: (a) The trapped C ion distribution as a function of energy ($\tilde{\phi} \sim 0.1$). (b) The relative amplitudes of the first and second harmonics of each mode. Below, the measured frequency shift of the (c) fast and (d) slow IAW modes compared to kinetic and fluid analytic calculations, where "sudden" and "adiabatic" refer to the excitation of the ions ($\alpha_{\mathrm{e}} = \alpha_{\mathrm{ad}}$).

the amplitude to which the wave was driven was varied to determine the dependence of $\delta\omega_{\mathrm{NL}}$ on ϕ (details of the signal processing techniques used are given in Ref. [9]). Two physically relevant, weakly-damped cases are presented here in detail: a fast mode, where $T_{\mathrm{i}}/T_{\mathrm{e}} = 0.07$, and a slow mode, where $T_{\mathrm{i}}/T_{\mathrm{e}} = 0.5$ (points C and B, respectively, in Fig. 1).

Figure 2 shows the distributions of the H ions, f_{H}, and C ions, f_{C}, for both modes. Figure 2c shows that while f_{H} is heavily modified, the particles are roughly evenly distributed across the trapping region. In contrast, the trapped C ions of the slow mode and H ions of the fast mode are concentrated at the separatrix, while there is little evidence of trapping of C ions of the fast mode. These numerically obtained distributions were compared with the analytic distributions f_{ad} and f_{sud} expected in the adiabatic and sudden excitation cases, respectively, using expressions given in Ref. [11], and are shown for the slow mode C ions in Fig. 3a. The analytic calculations were repeated using the actual ϕ taken from simulations rather than assuming a sinusoid (and therefore including the impact of harmonic generation); with the actual ϕ,

the agreement between the adiabatic model and the simulation is excellent for all species of both modes across all values of ϕ studied ($5 \times 10^{-3} \lesssim \tilde{\phi} \lesssim 0.1$).

Harmonic generation in IAWs has been the subject of many previous studies. Solving the homogeneous cold-ion fluid equations for an IAW including its harmonics (see, e.g., Pesme *et al.* [15]) results in a first harmonic ϕ_1 driving a second harmonic ϕ_2, scaling such that $|\phi_2| \sim |\phi_1|^2$, and a frequency shift of the fundamental $\delta\omega_{\rm NL}^{\rm flu}$ proportional to $|\phi_1|^2$. In Fig. 3b, measured ratios $|\phi_2|/|\phi_1|$ for the fast and slow modes are shown. In fact neither fast nor slow modes show the scaling expected from a cold-ion fluid model. Single-species studies of harmonic generation have also been found to diverge from this model [9].

Figures 3c and 3d show the measured deviation in frequency $\delta\omega_{\rm NL}$ from ω_0 as a function of ϕ (for Vlasov results, we measure $\omega_0 = \omega(\phi \to 0)$; for analytic calculations, $\omega_0 = \omega_R$). The observed trend of increasing frequency as a function of ϕ further supports the choice of the adiabatic limit of α_j in Eq. 4 for all species: using the sudden limit for the ions and an adiabatic limit for the electrons would imply an overall negative shift in frequency, contrary to what is observed in Vlasov simulations. In single-species plasmas, the sudden limit was found to better match Vlasov simulation results for ions at high $T_{\rm i}/T_{\rm e}$ [9]; we observe that whether the nonlinear response of a mode is better approximated by adiabatic or sudden ion excitation limits is determined not only by the rate of gain in ϕ compared to the ion bounce frequencies, but on the properties of the mode.

From these results, it is clear that calculations of $\delta\omega_{\rm NL}^{\rm kin}$ from Eq. 4 match Vlasov results well for low ϕ, but underestimate $\delta\omega_{\rm NL}$ at higher amplitudes where harmonic generation is expected to contribute a further positive frequency shift. The fluid shift is also shown using a cold ion model. While not formally consistent, a simple linear sum of the kinetic and fluid frequency shifts shows convincing agreement with Vlasov results for fast and slow modes in both magnitude and ϕ scaling.

In summary, the rich and differing nonlinear behaviours of the fast and slow IAW modes of CH plasma have been presented in detail for the first time in regimes relevant to current ignition experiments. Good agreement between multi-species analytic calculations of the nonlinear frequency and highly-resolved Vlasov simulations across the most physically relevant regimes is observed. Across the more weakly damped regimes for each mode, the overall positive sign of the frequency shift of the fast mode, and of the slow mode for $T_{\rm i}/T_{\rm e} \lesssim 0.6$, imply (I) the electron dynamics must be sufficiently resolved for all $T_{\rm i}/T_{\rm e}$ in order to accurately model nonlinear IAWs, and (II) both modes are susceptible to modulational instability of the type described in Ref. [16] over these ranges.

The authors gratefully acknowledge the helpful comments of B. I. Cohen and I. Y. Dodin, and the suggestions of the Referees. This work was performed under the auspices of the U.S. Department of Energy by Lawrence Livermore National Laboratory under Contract DE-AC52-07NA27344 and funded by the Laboratory Research and Development Program at LLNL under project tracking code 12-ERD-061.

* email: chapman29@llnl.gov

[1] J. D. Lindl *et al.*, Phys. Plasmas **11**, 339 (2004).
[2] D. S. Clark, S. W. Haan, B. A. Hammel, J. D. Salmonson, D. A. Callahan, and R. P. J. Town, Phys. Plasmas **17**, 052703 (2010).
[3] T. M. O'Neil, Phys. Fluids **8**, 2255 (1965).
[4] D. H. Froula, L. Divol, and S. H. Glenzer, Phys. Rev. Lett. **88**, 105003 (2002).
[5] F. Anderegg, C. F. Driscoll, D. H. E. Dubin, T. M. ONeil, and F. Valentini, Phys. Plasmas **16**, 055705 (2009).
[6] N. B. Meezan *et al.*, Phys. Plasmas **17**, 056304 (2010).
[7] E. A. Williams, R. L. Berger, R. P. Drake, A. M. Rubenchik, B. S. Bauer, D. D. Meyerhofer, A. C. Gaeris, and T. W. Johnston, Phys. Plasmas **2**, 129 (1995).
[8] F. Valentini, F. Califano, D. Perrone, F. Pegoraro, and P. Veltri, Phys. Rev. Lett. **106**, 165002 (2011) and references therein.
[9] R. L. Berger, S. Brunner, T. Chapman, L. Divol, C. H. Still, and E. J. Valeo, accepted and awaiting typesetting for Phys. Plasmas., reference number POP39701A.
[10] G. J. Morales and T. M. O'Neil, Phys. Rev. Lett., **28**, 417 (1972).
[11] R. L. Dewar, Phys. Fluids **15**, 712 (1972).
[12] C. Riconda, A. Heron, D. Pesme, S. Hüller, V. T. Tikhonchuk, and F. Detering, Phys. Rev. Lett. **94**, 055003 (2005).
[13] If instead of following the derivation found in Ref. [11] and Taylor expanding the H distribution around the phase velocity one finds the nonlinear part of the dispersion relation by numeric integration, the same result is obtained.
[14] I. B. Bernstein, J. M. Greene, and M. D. Kruskal, Phys. Rev. **108**, 546 (1957).
[15] D. Pesme, C. Riconda, and V. T. Tikhonchuk, Phys. Plasmas **12**, 092101 (2005).
[16] R. L. Dewar, W. L. Kruer, and W. M. Manheimer, Phys. Rev. Lett. **28**, 215 (1972).